Journal of Mathematical Chemistry 25 (1999) 295–308

Note

Continuous symmetry measures: A note in proof of the folding/unfolding method

Yair Salomon and David Avnir

Institute of Chemistry and The Lise Meitner Minerva Center for Computational Quantum Chemistry, The Hebrew University of Jerusalem, Jarusalem 91904, Israel
E-mail: david@chem.ch.huji.ac.il

Received 12 March 1999

The measurement of the degree of symmetry proved to be a useful tool in the prediction of quantitative structural–physical correlations. These measurements have been based, in the most general form, on the folding/unfolding algorithm, for which we provide here a new and simpler proof. We generalize this proof to the case of objects composed of more than one (full) orbit. An important practical issue we consider is the division of the graph into symmetry orbits and the mapping of the symmetry group elements onto the points of the graph. The logical constraints imposed by the edges of the graph are reviewed and used for the successful resolution of the coupling between different orbits.

1. Background: The measurement of symmetry by the "folding–unfolding" approach

The measurement of the degree of symmetry content of structures [1,2,4,5,9–12,20] proved to be useful in the elucidation of quantitative correlations between physical [3,5,6,15], chemical [7,14], biochemical [8,19] and even archeological [18] observables and symmetry. It is a new approach which, we believe, carries much potential in better understanding of problems of structural chemistry. It therefore needs continuous improvements, additions of computational tools and better proofs as to their task of providing the global minimum solutions. This is the topic of this report; it concentrates on the "folding–unfolding" (FU) algorithm (desribed below) which was devised to provide a minimal solution to the following definition of the symmetry measure:

$$S(G) = \frac{1}{N\alpha} \sum_{j=1}^{N} \left(p_j - \widehat{p}_j\right)^2. \tag{1}$$

Here, $p_1, \ldots, p_N$ are the vertices of the original graph (V, E) embedded in the Euclidean space and used to represent a structure of interest, $\widehat{p}_1, \ldots, \widehat{p}_N$ are the vertices of a G-symmetric graph with the same connectivity as the original one, N is the number of graph points and α is a size normalization factor, taken as either the maximal

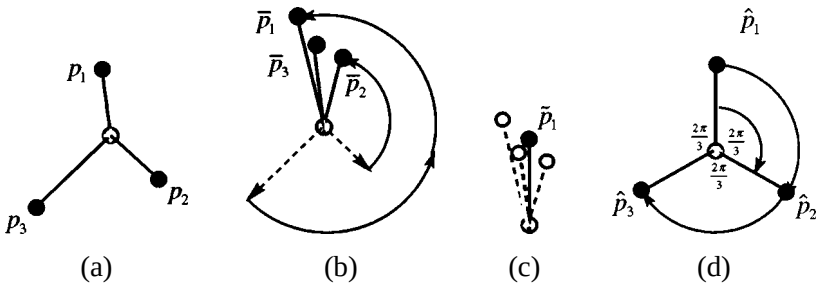

Figure 1. An illustration (adapted from [21]) of the folding/unfolding method. Given a mapping of the group elements onto the points of the object (a) ($e \rightarrow p_1$, $c_3 \rightarrow p_2$, $c_3^2 \rightarrow p_3$), the points are folded by applying the inverse element on the points (b), the resulting cluster is averaged (c), and unfolded (d) by applying the proper symmetry element.

distance from the center of mass to the farthest vertex [22] or as the r.m.s. distance of all vertices from that center.[1]

The task has been then to find the closest G-symmetric graph, $\widehat{p}_1, \ldots, \widehat{p}_N$, to the original graph $p_1, \ldots, p_N$, such that $S(G)$ is minimal. The FU algorithm, which was designed to solve this problem and is described in detail below, is exemplified in figure 1: each point of the graph is mapped to an element g of G, the symmetry group, bundling points into induced orbits. Each point is transformed under g^{-1} (folded) creating clusters that are averaged and unfolded (transformed under g) to form the closest symmetric graph. A proof that the FU algorithm indeed leads to the minimal $S(G)$ was derived using Lagrange multipliers [22]. The FU method is general, but it implicitly assumes that the reference frame of the symmetric operation is known i.e., that the orientation of the symmetry elements relative to the object is known. In some cases, closed-form solutions for the orientation of the symmetry elements were obtained (e.g., [17,23]); in others, iterative minimization procedures are used (e.g., C_n, $n > 2$, symmetry in 3D). Another computational approach was developed recently, tailored to the problem of finding the minimal distance of a given structure to a desired general shape with the same number of vertices. That approach is general from a point of view not shared with the FU algorithm: it allows one to determine the distance from any required shape, symmetric or not, and is based solely on the minimization of relative size and mutual orientation between the original structure and the target shape [13].[2] It solved a problem encountered with the FU approach, namely that for multiple vertices structures with highly connected graphs such as the polyhedra, the computation quickly becomes cumbersome for reasons we

[1] We represent an object (a molecule in most cases) by a graph, (V, E), embedded in the Euclidean space and a weight distribution function (DF), $\rho(p_j) = \omega_j$. For simplicity of notation, we discuss only the uniform DF, $\rho(p_j) = 1/N$, as the derivation below can be easily generalized to any DF. It should be emphasized that the weight of the DF is concentrated solely at the vertices of the graph and that the edges represent only logical relations between the vertices.

[2] Interestingly, this approach links the continuous symmetry measure as expressed by equation (1) with the correlation coefficient probability measure of having a specific symmetry.

discuss below (see section 3.1). Yet the FU algorithm remains at the moment the most general approach, and hence we resort to its further perfection: we provide here a simpler proof that the FU algorithm leads to the minimal $S(G)$ and generalize it to the case where the object is decomposed into more than one (full) induced orbit; and we discuss the role of the logical symmetry of the graph.

2. Proof that the folding–unfolding algorithm leads to the minimal value of the symmetry measure

2.1. Introductory comments: The division of the graph into orbits

A symmetric object is invariant under symmetry operations and the points of the symmetric object divide into closed sets, *orbits*, where a point in an orbit transforms by a symmetry operation into another point in the same orbit. This does not apply to the pre-symmetrized object, but the bijective (one-to-one) mapping between the points (and edges) of the pre-symmetrized and the symmetrized objects induces a division of the pre-symmetrized object into *induced orbits*. Furthermore, the symmetry group defines relations between the points of the symmetric object which might be viewed as a mapping of the group elements onto the orbit's points. These relations are induced onto the pre-symmetrized object as well and define an internal ordering of the points of the pre-symmetrized object. The number of possible divisions of the graph into induced orbits is finite, and so is the number of possible mappings of the group elemets onto each orbit. Therefore, in principle, it is possible to find the closest symmetric object for every such division and internal ordering. However, one has to take into account the relations between the elements of the symmetry group as well. These are most clearly studied by examining the closest symmetric orbit $\widehat{p}_1, \ldots, \widehat{p}_k$, where k is the size of H, a subgroup of G. Indeed, the definition of a *partial orbit* is its invariance under the operations of H. The relations between the points of the orbit are

$$\widehat{p}_1 = f_1(\widehat{p}_1), \qquad \widehat{p}_2 = f_2(\widehat{p}_1), \qquad \ldots, \qquad \widehat{p}_k = f_k(\widehat{p}_1), \tag{2}$$

where $f_1, \ldots, f_k$ are the elements of H and f_1 is the identity operation. The points $\widehat{p}_1, \ldots, \widehat{p}_k$ have a nontrivial *stabilizer*. (The stabilizer of a point x is the set of the symmetry operations of G under which operation it is invariant, i.e., $\{g \in G \mid g(x) = x\}$.) Denoting the elements of the stabilizer by $s_1, \ldots, s_d$ (s_1 is again the identity) we may write down the operations of G in the following manner:

$$G = \begin{Bmatrix} s_1 f_1, & s_1 f_2 & \cdots & s_1 f_k, \\ s_2 f_1, & s_2 f_2 & \cdots & s_2 f_k, \\ \vdots & \vdots & \vdots & \vdots \\ s_d f_1, & s_d f_2 & \cdots & s_d f_k \end{Bmatrix}. \tag{3}$$

Every row is a class of G and every operation in the ith column translates $\widehat{p}_1$ to $\widehat{p}_i$. A 2D example is the equilateral triangle graph. The points of that graph define an orbit under the operations of the C_3 group, which is a subgroup of D_3. Here, e (the

identity) and σ (a reflection through a line passing through one of the vertices and the mass center) compose the stabilizer:

$$D_3 = \begin{Bmatrix} e, & c_3, & c_3^2, \\ \sigma, & \sigma c_3, & \sigma c_3^2 \end{Bmatrix}. \tag{4}$$

The internal order between the points of a partial orbit can be determined by the internal order of the operations of H. Grouping the symmetry operations of G by the columns of equation (3) we get the following identities:

$$\begin{aligned} \widehat{p}_1 &= g_i(\widehat{p}_1), \quad i = 1, \ldots, d, \\ \widehat{p}_2 &= g_i(\widehat{p}_1), \quad i = d+1, \ldots, 2d, \\ &\vdots \\ \widehat{p}_k &= g_i(\widehat{p}_1), \quad i = (k-1)d+1, \ldots, kd = m; \end{aligned} \tag{5}$$

if $i = d(x-1) + y$ ($1 \leqslant x \leqslant k$, $1 \leqslant y \leqslant d$), then $g_i = s_y f_x$.

Duplicating $\widehat{p}_1, \ldots, \widehat{p}_k$ orbit d times we may define a bijective mapping of the G onto the duplicated orbit,

$$d \cdot \widehat{O} = \{ \underbrace{\widehat{p}_1, \ldots, \widehat{p}_1}_{d}, \underbrace{\widehat{p}_2, \ldots, \widehat{p}_2}_{d}, \ldots, \underbrace{\widehat{p}_k, \ldots, \widehat{p}_k}_{d} \},$$

according to equation (3). In its turn a bijective mapping of the operations of G onto the duplicated induced orbit,

$$d \cdot O = \{ \underbrace{p_1, \ldots, p_1}_{d}, \underbrace{p_2, \ldots, p_2}_{d}, \ldots, \underbrace{p_k, \ldots, p_k}_{d} \},$$

can be inferred by the same rule. We return to these issues in the discussion.

2.2. Proof that the mass centers of the original and symmetrized structures coincide

We prove first that, in order for equation (1) to provide the minimal S value, the mass centers of the original object, $\omega = (1/N)\sum_{j=1}^{N} p_j$, and of the symmetrized object, $\widehat{\omega} = (1/N)\sum_{j=1}^{N} \widehat{p}_j$, should coincide. Assuming the contrary we have $\omega - \widehat{\omega} = \varepsilon \neq 0$. Without loss of generality we may assume that $\widehat{\omega} = 0$ and then $(1/N)\sum_{j=1}^{N} \widehat{p}_j = \varepsilon$. It turns out that the object $P' = \{\widehat{p}_1 + \varepsilon, \ldots, \widehat{p}_N + \varepsilon\}$ is closer to the original object:

$$\begin{aligned} S(P) - S(P') &= \frac{1}{N}\sum_i \left(p_i - \widehat{p}_i\right)^2 - \frac{1}{N}\sum_i \left(p_i - \left(\widehat{p}_i + \varepsilon\right)\right)^2 \\ &= \frac{2\varepsilon}{N}\sum_i p_i - \varepsilon^2 = \varepsilon^2 > 0, \end{aligned} \tag{6}$$

a contradiction to the assumption that $\widehat{\omega}$ is the mass center of the closest symmetric object.

The constraint on the mass center of the closest symmetric object is the basic coupling between the different orbits. A variation of the location of a point in one orbit varies the location of the mass center through which all symmetry elements pass and, therefore, has an effect on all of the points of the object. It should be noted that for some symmetries (e.g., inversion and C_n in 2D) the mass center is all that is needed to determine the orientation of the symmetry elements and the calculation for the different orbits is totally separable.

2.3. *Proof of the FU algorithm*

We begin with a full induced orbit, $p_1, \ldots, p_m$ (where m is the size of G), and, as explained above, we search for the closest symmetric orbit $\widehat{p}_1, \ldots, \widehat{p}_m$. The symmetry of $\widehat{p}_1, \ldots, \widehat{p}_m$ is made explicit by writing down the relations between the points in term of the symmetry operations:

$$\widehat{p}_1 = \widehat{p}_1, \qquad \widehat{p}_2 = g_2(\widehat{p}_1), \qquad \ldots, \qquad \widehat{p}_m = g_m(\widehat{p}_1). \tag{7}$$

As the symmetry operations are distance preserving, we have

$$S = \frac{1}{m}\sum_i \left(p_i - \widehat{p}_i\right)^2 = \frac{1}{m}\sum_i \left(g_i^{-1}(p_i) - g_i^{-1}(\widehat{p}_i)\right)^2 = \frac{1}{m}\sum_i \left(g_i^{-1}(p_i) - \widehat{p}_1\right)^2. \tag{8}$$

It turns out that the only unknown is $\widehat{p}_1$, but the closest point (by mean squares) to a cluster is its average and, therefore, $S(G)$ is minimized when $\widehat{p}_1 = (1/m)\sum_i g_i^{-1}(p_i)$. The other points $\widehat{p}_2, \ldots, \widehat{p}_m$ are given by equation (7).

We have thus found a formula for the calculation of the closest symmetric orbit. We have also made explicit the mapping of the group elements onto the points of the induced orbit: $g_j \leftrightarrow \widehat{p}_j \leftrightarrow p_j$. We may reverse our argument and deduce the internal ordering of the symmetric orbit by a mapping of the group elements onto the induced orbit. Searching through all the possible internal orderings of $p_1, \ldots, p_m$, i.e., the (bijective) mapping of g_k onto p_j, one finds the closest symmetric (full) orbit.

The extension of the proof for partial orbits, following the above introductory comments, becomes straightforward: the same steps are followed, except that, since we duplicated the orbit by d (the size of the stabilizer), we divide the sum of squares by d:

$$S = \frac{1}{d \cdot f}\sum_i \left(p_i - g_i(\widehat{p}_1)\right)^2 = \frac{1}{m}\sum_i \left(g_i^{-1}(p_i) - \widehat{p}_1\right)^2. \tag{9}$$

Note that $\{p_i\}$ is the duplicated set of points according to equation (5). Again, $\widehat{p}_1$ is the only unknown and minimization is achieved when $\widehat{p}_1 = (1/m)\sum_i g_i^{-1}(p_i)$.

Concluding the proof we note that although $\widehat{p}_1$ is an average of a cluster of the size of G where all the elements of G are used in the folding process, the unfolding is achieved by the operation of the elements of H alone:

$$\widehat{p}_i = f_i(\widehat{p}_i), \quad i = 1, \ldots, k. \tag{10}$$

3. Discussion and comments on the proof

3.1. The division of the graph into orbits

The proof provided in section 2 requires some further comments and clarifications, which we address in this section. The first refers to the question of finding the proper internal orderings and divisions of the graph. We first examine the question of finding a proper internal ordering for one orbit and then generalize the procedure to manage the division into several (induced) orbits as well. Our proof of the folding/unfolding method has emphasized the relation between the points of an orbit (or better, the points of an induced orbit) and the group elements. The question that arises is, how to find the mapping of the group elements onto the induced orbit that minimizes S? Scanning over the possible mappings of the group elemets onto the points of an induced orbit is simplified if we note that one set can be held in constant order (e.g., the points), while the other set is permuted. The reason this is true is that only the internal order in which the points of the induced orbit are folded is important. Consider, for example, a full orbit. We show that two mappings of G onto $p_1, \ldots, p_m$ are equivalent if they are shifted by g_α (an operation of G), i.e., we show that by mapping $g_1 \rightarrow p_1$, $g_2 \rightarrow p_2$, $\ldots$, $g_m \rightarrow p_m$ and by mapping $g_\alpha g_1 \rightarrow p_1$, $g_\alpha g_2 \rightarrow p_2$, $\ldots$, $g_\alpha g_m \rightarrow p_m$, the same symmetric object is obtained.

By application of the folding step in the first case, $\widehat{p}_1$ is calculated: $\widehat{p}_1 = (1/m)\sum_i g_i^{-1}(p_i)$. It is enough to show then that the same expression is obtained in the second case. This is done as follows: note that, in the first case, $\widehat{p}_1$ is the point closest to p_1, the point onto which the identity operation is mapped. In the second case, $\widehat{p}_1$ is the point, which we denote as $\widehat{p}_\alpha$, which is closest to p_α, the point onto which g_α^{-1} is mapped in the first case. Thus, denoting $g_i g_\alpha$ by f_i, the expression in the second case is

$$\widehat{p}_\alpha = \frac{1}{m}\sum_{i=1}^{m} f_i^{-1}(p_i) = \frac{1}{m}\sum_{i=1}^{m} g_\alpha^{-1} g_i^{-1}(p_i) = g_\alpha^{-1}\frac{1}{m}\sum_{i=1}^{m} g_i^{-1}(p_i) \qquad (12a)$$

or

$$\widehat{p}_\alpha = g_\alpha^{-1}\widehat{p}_1, \qquad (12b)$$

and we have shown that $\widehat{p}_\alpha$ is the point which is closest to p_α, the point onto which g_α^{-1} was mapped in the first case. The generalization to the partial orbit case is along the same lines as in the proof of the previous section.

Having proved that one set (the group elemets or the points) may be held constant, we address the question which constraints are imposed on these mappings by the graph. Choosing to hold the operation of the group constant, the different mappings of G onto an orbit may be viewed as placing the points of the orbit into bins – the different group elements. Searching over all the mappings of the group elements onto the points of an orbit is therefore analogous to checking all the permutations of points of the orbit. This point of view can be applied to the general case where the object is divided into several

(induced) orbits. Since permutations can be treated as internal mappings of the graph – permutations may always be expressed as cycles – the problem is reduced to finding the internal mappings of the graph, constrained by two considerations: graph constraints and symmetry constraints: a point is permuted to another one only if it is totally equivalent. The graph constraints a mapping $p_j \rightarrow p_k$ to be proper only if, for every pair (p_j, p_k), p_j and p_k have the same number of edges and only if each neighbor of p_j is properly mapped to a neighbor of p_k. To study the symmetry constraints recall that saying that a graph is G-symmetric is equivalent to saying that the application of every element g_k of G on the graph implies a change of labeling of the graph: for every vertex p_j and every edge (p_i, p_j), there are vertex $g_k(p_j)$ and edge $g_k(p_i, p_j) = (g_k(p_i), g_k(p_j))$. Such a permutation does not change any feature of the graph.

Two comments are in order here. First, edges connecting vertices within an orbit always satisfy the above relations/constraints. Second, not all edges (connecting different orbits) have to be checked. As we will see below this check may sometimes be reduced to a compact form. An example is the C_n symmetry case, where the edges connecting different orbits need not be checked at all! This is due to the fact that different orbits are coupled only by the symmetry axis of rotation. In such cases, the validation of the division to orbits reduces into checking that these divisions are of the size of an orbit. In other cases (cf. section 3.2), the validation of the symmetry of the edges requires the explicit examination of existence of $g_k(p_i, p_j) = (g_k(p_i), g_k(p_j))$ at least for a reduced set of operations. Coupling and its consequence will be discussed in the next section.

The set of proper internal mappings can be extracted by a recursive precedure, testing at each consequent step whether a mapping is proper. As the graph is finite, the process would either end with a proper mapping or reach a dead end where none of the unmapped points has a proper match. In this case, the process will return to a previous step, searching for another mapping. Table 1 summarizes the procedure in pseudo-code. The search over the set of permutation (or automorphisms of graph) seems a demanding task, but is greatly simplified using the information encoded in the edges of the graph. The general equivalence between points of the graph can be determined by the relatively fast procedure of Rucker et al. [16]. Indeed, if the graph has no edges, all points are equivalent and all permutations are permitted by the graph. It should be emphasized that such cases rarely occur in practical problems. Highly connected graphs pose the same problems, since there are many options at each stage of the recursion. In the case of the classical polyhedra, another computational approach is given in [13]. Given the general scheme of the procedure of the mapping of the group operations onto the points of the graph we now discuss the question of coupling between orbits.

3.2. The coupling between orbits

As noted above, in some cases, the coupling between orbits is restricted to variation of the location of their mass centers, and, therefore, the calculation is separated

Table 1
Pseudo-code for the mapping procedure.

```
//Given a graph G(V, E), build all the possible permutations of equivalent vertices according
to the symmetry group and other related data.
//----------The initializing step----------
permute(vertex 0, graph G, array permutation)
//----------The basic function----------
permute(vertex i, graph G, array permutation)
{
  while (not all possibilities were extracted)
    {find j, the next possible equivalent vertex of vertex i, according to rules 1–5 (below)
     permute(j, G, permutation)}
  (end while)
  back up one level (if it was vertex 0, then exit)
}
//----------
The rules by which vertex j may or may not match vertex i:
  1. A cycle of the permutation must be of the size of a subgroup of the symmetry group
     specified.
  2. Equivalent vertices must have the same color (type).
Two vertices (i, j) may permute if:
  3. They have the same valency (coordination).
  4. Each neighbor of i is mapped onto a neighbor of j.
  5. If a neighbor of i is not matched yet, then j has a neighbor that may be a possible match
     for that neighbor of i.
```

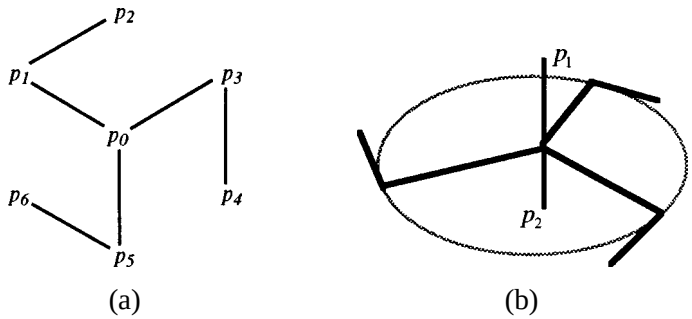

Figure 2. (a) The 2D triskelion, a C_3 symmetric object used in the text. (b) A 3D variant of the triskelion that has an additional two-point orbit (points p_1 and p_2).

to the different orbits. An example that will further clarify the coupling of orbits is the calculation of the closest D_n symmetric object in 2D, taking as a particular case the C_3-symmetric triskelion (figure 2(a)). For the calculation of S (D_n, $n = 3$ in this case), we use a generalization of the solution given in [23], described in the appendix.

The solution to the D_n problem illustrates the way constraints imposed by the edges of the graph and the group symmetry should be taken into account. We develop our example in 2D, but as the following can be generalized to three dimensions, we denote the σ operations as c_2 operations orthogonal to the main rotation axis or c_2^+.

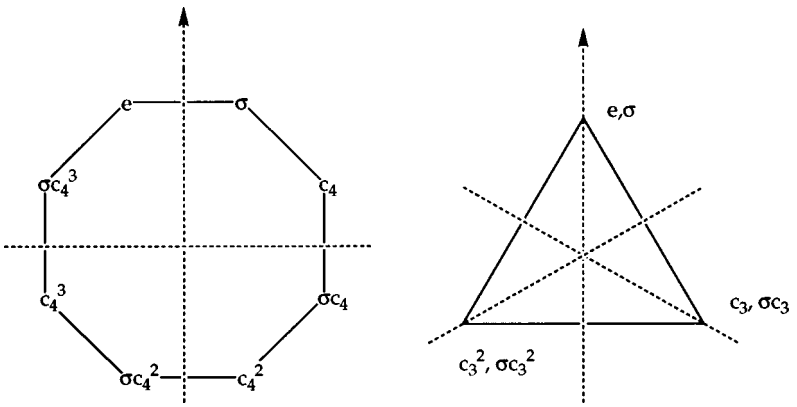

Figure 3. An illustration of the relation between the elements of the D_n symmetry group: (a) in the case of a full orbit, (b) in the case of a partial n-orbit (cf. equations (15) and (16)).

First we consider the possible mapping of the group elements onto a D_n symmetric object and then, as usual, we induce these mappings onto the pre-symmetrized object. The different orbits are coupled by the c_2^+ operations: given a D_n symmetric object and an edge of the graph $e(i,j)$, then for every c_2^+ symmetry element (orthogonal to the main rotation axis) there exists a c_2^+symmetric edge $e(c_2^+(i), c_2^+(j))$ such that $e(c_2^+(i), c_2^+(j)) = c_2^+[e(i,j)]$, i.e., the c_2^+ rotated edge is the edge connecting the c_2^+ rotated points. The whole process of symmetrization is formulated in terms of operations on the points of the graph, therefore we wish to formulate this constraint in these terms as well. To make the formulation clearer we denote each point of an orbit by a representative element of the symmetry group that is mapped onto it. Thus, in the case of a full (induced) orbit, the point onto which the c_n^i is mapped is denoted by $\underline{c_n^i}$. In the case of a partial orbit of n vertices, $c_2^+ c_n^i$ is mapped onto the point as well. As a convention, we will denote this point again by $\underline{c_n^i}$. We may now write the constraints in terms of constraints on the vertices of the graph. These constraints are illustrated in figure 3(a) and (b) for the full and n-orbit, respectively. In the case of a full (induced) orbit,

$$c_2^+\left(\underline{c_n^i}\right) = \underline{c_2^+ c_n^{n-i}}, \tag{15}$$

i.e., the operation of the c_2^+ element on the point onto which the c_n^i is mapped transforms it to the point onto which the $c_2^+ c_n^{n-i}$ element is mapped. From the fact that $(c_2^+)^2 = e$, we conclude that

$$c_2^+\left(\underline{c_2^+ c_n^i}\right) = \underline{c_n^{n-i}}.$$

In the case of a partial orbit of n vertices, the constraint is reduced to

$$c_2^+\left(\underline{c_n^i}\right) = \underline{c_n^{n-i}}. \tag{16}$$

Two trivial cases are left: the first is the case of a singleton. In this case, the question onto which point of the orbit a group element is mapped under the c_2^+ transformation is meaningless, as all group elements are mapped onto the same point. The second case is a two-point orbit occurring, for example, in figure 2(b), a 3D variation of a triskelion. In this case, the mapping of the group elements is $e, c_n, c_n^2, \ldots, c_n^{n-1} \rightarrow p_1$ and $c_2^+, c_2^+c_n, c_2^+c_n^2, \ldots, c_2^+c_n^{n-1} \rightarrow p_2$ and, therefore,

$$c_2^+\left(\underline{c_n^i}\right) = \underline{c_2^+c_n^{n-i}},$$

i.e., edges connected to p_1 are transformed onto edge connected to p_2. In the passing we note that figure 2(b) was used by Moreau [12] as an example where his method of averaging local chirality contributions to a global chirality measure does not identify the chirality of objects from this family; the continuous symmetry measure approach is devoid of this problem.

Finally, one should note that edges that connect points within the same orbit need not be checked as they connect totally equivalent points, and, therefore, every such edge transforms to an equivalent edge. We conclude this section by noting that, though the edges of the graph are "weightless", they still affect the way the CSM is assessed and that the information encoded by the edges can be efficiently used by selection of the proper coupling between the points of the graph.

In summary, we have presented a simplification and generalization of the proof of the folding unfolding method and addressed the question of coupling between different induced orbits. In our formalism, the logical role of the edges in the graph model is emphasized: the symmetry of edges is deduced from the symmetry of the points they connect and used to constrain the allowed internal maps of the graph.

Appendix. Calculation of best orientation of the D_n elements in 2D

The problem. As noted above, there is a difficulty with the folding/unfolding method which does not determine explicitly the best orientation of the symmetry elements relatively to the pre-symmetrized object. In this appendix we exemplify a method for the determination of the orientation of these elements for the 2D case. Thus, we provide a generalization of [23] which dealt only with the case of full orbits. To make the derivation simpler, we begin with the simple case of the calculation of the orientation of the 2D D_1 symmetry (= 2D reflection symmetry) and use it as a leverage for the more general solution.

(i) 2D reflection symmetry. In this simple case – the degenerate D_n problem – the only c_n element is the identity. Therefore the division of the graph is into two sets only: points folded by the reflection element and points that the identity is mapped onto them (and are not reflected).

Our aim is the calculation of θ, the angle of the reflection axis relative to the x–y coordinates of the pre-symmetrized object, such that minimizes $S = (1/N)\sum_i (p_i - \widehat{p}_i)^2$

or $\widetilde{S} = \sum_i (p_i - \widehat{p}_i)^2$. These expressions consist of two contributions: the sum over the full orbits (two-point orbits) and the sum over the singletons. Thus, one has to minimize

$$\widetilde{S} = \sum_{\text{pairs}} \left[\left(p_{i1} - \widehat{p}_{i1}\right)^2 + \left(p_{i2} - \widehat{p}_{i2}\right)^2 \right] + \sum_{\text{singletons}} \left(p_i - \widehat{p}_i\right)^2. \tag{A.1}$$

The folding/unfolding method gives the expression for $\widehat{p}_i$ (in the singleton case) and for $\widehat{p}_{i1}$ and $\widehat{p}_{i2}$ (in the two-point orbit case) in terms of p_i and of p_{i1} and p_{i2}, respectively. After substitution of these expressions in equation (A.1) and a little algebra we get

$$\widetilde{S} = \frac{1}{2} \sum_{\text{pairs}} \left[p_{i1}^2 + p_{i2}^2 - 2 p_{i1} \sigma(p_{i2}) \right] + \frac{1}{2} \sum_{\text{singletons}} \left[p_i^2 - p_i \sigma(p_i) \right]. \tag{A.2}$$

Taking the derivative of this expression with respect to θ, the terms independent of θ may be dropped:

$$\frac{\mathrm{d}\widetilde{S}}{\mathrm{d}\theta} = \frac{\mathrm{d}}{\mathrm{d}\theta} \sum_{\text{pairs}} \left[-p_{i1} \sigma(p_{i2}) \right] + \frac{1}{2} \frac{\mathrm{d}}{\mathrm{d}\theta} \sum_{\text{singletons}} \left[-p_i \sigma(p_i) \right]. \tag{A.3}$$

Writing down the explicit expression for the reflection matrix and the points of the object by their coordinates we have

$$\sigma(p_i) = \sigma \begin{bmatrix} x \\ y \end{bmatrix} = \begin{bmatrix} x \cos(2\theta) + y \sin(2\theta) \\ x \sin(2\theta) - y \cos(2\theta) \end{bmatrix} \tag{A.4}$$

and

$$\begin{aligned} \frac{\mathrm{d}\widetilde{S}}{\mathrm{d}\theta} = & -\frac{\mathrm{d}}{\mathrm{d}\theta} \sum_{\text{pairs}} \left[x_{i1} \left(x_{i2} \cos(2\theta) + y_{i2} \sin(2\theta) \right) + y_{i1} \left(x_{i2} \sin(2\theta) - y_{i2} \cos(2\theta) \right) \right] \\ & - \frac{1}{2} \frac{\mathrm{d}}{\mathrm{d}\theta} \sum_{\text{singletons}} \left[x_i \left(x_i \cos(2\theta) + y_i \sin(2\theta) \right) + y_i \left(x_i \sin(2\theta) - y_i \cos(2\theta) \right) \right]. \end{aligned} \tag{A.5}$$

Equating this expression to zero we get

$$\tan(2\theta) = \frac{2 \sum_{\text{pairs}} [x_{i1} y_{i2} + x_{i2} y_{i1}] + 2 \sum_{\text{singletons}} x_i y_i}{2 \sum_{\text{pairs}} [x_{i1} x_{i2} - y_{i1} y_{i2}] + \sum_{\text{singletons}} [x_i^2 - y_i^2]}. \tag{A.6}$$

(ii) 2D D_n symmetry. The next goal is the calculation of the reflection lines in the D_n case. Here, the c_n elements are involved in the calculation, and our aim is to eliminate this extra complication and to reduce it to the previous simpler case. Since, as shown above, the mass center is one point through which the reflection lines must pass, it is the point which determines the main axis of rotation. The lines of reflection are set $2\pi/n$ apart, and, therefore, it is enough to determine one of them, which we designate by σ. As we shall see below, the analogy to the simple case is achieved by collecting the elements of the minimization equation by the elements of the partial symmetry

group C_n. The resulting expression is formally close to the folding expression. First, we define some notation. The elements of the symmetry group are

$$D_n = \begin{Bmatrix} e, & c_n, & c_n^2, & \ldots, & c_n^{n-1}, \\ \sigma, & \sigma c_n, & \sigma c_n^2, & \ldots, & \sigma c_n^{n-1} \end{Bmatrix}. \tag{A.7}$$

Indexing the points of an induced orbit by the mapping of the elements of the symmetry group onto the orbit, the point mapped onto c_n^j is p_{2j+1}, $j = 0, \ldots, n-1$, and the point mapped onto σc_n^j is p_{2j+2}, $j = 0, \ldots, n-1$. Noting that $(\sigma c_n^j)^{-1} = \sigma c_n^{-j}$, we first derive an expression for $\widehat{p}_1$ for different types of orbits beginning with the full $(2n)$ orbit:

$$\widehat{p}_1 = \frac{1}{2n}\left[\sum_{j=0}^{n-1} c_n^{-j} p_{2j+1} + \sigma \sum_{j=0}^{n-1} c_n^{-j} p_{2j}\right] = \frac{1}{2n}(T_1 + \sigma T_2), \tag{A.8}$$

where

$$T_1 \equiv \sum_{j=0}^{n-1} c_n^{-j} p_{2j+1}, \qquad T_2 \equiv \sum_{j=0}^{n-1} c_n^{-j} p_{2j}.$$

A similar expression is derived for the n-orbit case. The partial symmetry group in this case is C_n and the stabilizer is $\{e, \sigma\}$; the expression for $\widehat{p}_1$ can be written as a sum of two contributions:

$$\widehat{p}_1 = \frac{1}{2n}\left[\sum_{j=0}^{n-1} c_n^{-j} p_j + \sigma \sum_{j=0}^{n-1} c_n^{-j} p_j\right] = \frac{1}{2n}(T + \sigma T), \tag{A.9}$$

where $T \equiv \sum_{j=0}^{n-1} c_n^{-j} p_j$ is the C_n folded set of points.

Two cases are left – the singleton and pair orbits. However, these do not affect the orientation of the reflection lines, as, regardless of what is the orientation the points of the closest symmetric object belonging to such orbits, they will be located at the mass center. Therefore we need not include such points in the calculation. The contribution of different orbits to $\widetilde{S}$ is $\sum_{j=1}^{2n} p_j^2 - 2n\widehat{p}_i^2$ in the case of a full orbit and $\sum_{j=1}^{n} p_j^2 - n\widehat{p}_i^2$ in the case of an n-orbit. Therefore

$$\widetilde{S} = \sum_{2n\text{-orbits}} \left[\sum_{j=1}^{2n} p_j^2 - 2n\widehat{p}_i^2\right] + \sum_{n\text{-orbits}} \left[\sum_{j=1}^{n} p_j^2 - n\widehat{p}_i^2\right]. \tag{A.10}$$

The dependency of $\widetilde{S}$ on σ is given by the expressions for $\widehat{p}_{i1}$ (i is the index of the different orbits):

$$\frac{\mathrm{d}\widetilde{S}}{\mathrm{d}\theta} = -2n\frac{\mathrm{d}}{\mathrm{d}\theta} \sum_{2n\text{-orbits}} \widehat{p}_{i1}^2 - n\frac{\mathrm{d}}{\mathrm{d}\theta} \sum_{n\text{-orbits}} \widehat{p}_{i1}^2$$

$$= -2n\frac{\mathrm{d}}{\mathrm{d}\theta}\sum_{2n\text{-orbits}}\frac{1}{4n^2}(T_{i1}+\sigma T_{i2})^2 - n\frac{\mathrm{d}}{\mathrm{d}\theta}\sum_{n\text{-orbits}}\frac{1}{4n^2}(T_i+\sigma T_i)^2$$

$$= -\frac{1}{2n}\frac{\mathrm{d}}{\mathrm{d}\theta}\sum_{2n\text{-orbits}}(T_{i1}+\sigma T_{i2})^2 - \frac{1}{4n}\frac{\mathrm{d}}{\mathrm{d}\theta}\sum_{n\text{-orbits}}(T_i+\sigma T_i)^2. \qquad \text{(A.11)}$$

Equating to zero and multiplying by $2n$ we arrive at an expression similar to equation (A.3) where, instead of p_i, p_{i1} and p_{i2}, we have T_i, T_{i1} and T_{i2}:

$$\frac{\mathrm{d}\widetilde{S}}{\mathrm{d}\theta} = 0 = -\frac{\mathrm{d}}{\mathrm{d}\theta}\sum_{2n\text{-orbits}}[T_{i1}\sigma T_{i2}] - \frac{1}{2}\frac{\mathrm{d}}{\mathrm{d}\theta}\sum_{n\text{-orbits}}[T_i\sigma T_i]. \qquad \text{(A.12)}$$

Therefore an expression similar to equation (A.6) will give the orientation of σ, where the x's and y's are the coordinates of the T's. The alignment of the other reflection lines is immediately deduced, taking $\sigma_k = c_n^k\sigma$.

Acknowledgement

We thank H. Zabrodsky Hel-Or for critical reading of the manuscript and for important comments.

References

[1] D. Avnir, O. Katzenelson, S. Keinan, M. Pinsky, Y. Pinto, Y. Salomon and H. Zabrodsky Hel-Or, in: *Concepts in Chemistry: A Contemporary Challenge*, eds. D.H. Rouvray and E. Kirby (Research Studies Press, Somerset, 1996) pp. 283–324.
[2] D. Avnir, H. Zabrodsky Hel-Or and P.G. Mezey, Continuous symmetry and chirality measures, in: *Encyclopedia of Computational Chemistry*, Vol. 4, ed. P. von Rague Schleyer (Wiley, Chichester, 1998) pp. 2890–2901.
[3] V. Buch, E. Gershgoren, H. Zabrodsky and D. Avnir, Chem. Phys. Lett. 247 (1995) 149–153.
[4] R. Cammi and E. Cavalli, Acta Cryst. B 48 (1992) 245–252.
[5] C. Grimme, Chem. Phys. Lett. 297 (1998) 15–21.
[6] O. Katzenelson, H. Zabrodsky Hel-Or and D. Avnir, Chem. Eur. J. 2 (1996) 174–181.
[7] S. Keinan and D. Avnir, J. Am. Chem. Soc. 120 (1998) 6152–6159; http://chem.ch.huji.ac.il/∼david/shahar/QSAR/qsar.html.
[8] S. Keinan, J. Edelstein, M. Plato, M. Pinsky and D. Avnir, Chem. Phys. Lett. 298 (1998) 43–50.
[9] V.E. Kuzmin, I.B. Stelmakh, M.B. Bekker and D.V. Pozigun, J. Phys. Org. Chem. 5 (1992) 295–298.
[10] A.Y. Meyer and W.G. Richards, J. Comput. Aided Mol. Design 5 (1991) 427–439.
[11] P.G. Mezey, J. Am. Chem. Soc. 112 (1990) 3791–3802.
[12] G. Moreau, J. Chem. Inf. Comput. Sci. 37 (1997) 929–938.
[13] M. Pinsky and D. Avnir, Inorg. Chem. 37 (1998) 5575–5582.
[14] Y. Pinto, P.W. Fowler, D. Mitchell and D. Avnir, J. Phys. Chem. 102 (1998) 5776–5784.
[15] Y. Pinto, H. Zabrodsky Hel-Or and D. Avnir, J. Chem. Soc. Faraday Trans. 92 (1996) 2523.
[16] G. Rucker and C.J. Rucker, Chem. Inf. Comput. Sci. 30 (1990) 187–191.
[17] Y. Salomon and D. Avnir, J. Comput. Chem. 20 (1999) 772–780.
[18] I. Saragusti, I. Sharon, O. Katzenelson and D. Avnir, J. Archeol. Sci. 25 (1998) 817.
[19] A. Seri-Levy and W.G. Richards, Tetrahedron: Asymmetry 4 (1993) 1917–1923.

[20] N. Weinberg and K. Mislow, J. Math. Chem. 17 (1995) 35–53.
[21] H. Zabrodsky and D. Avnir, Adv. Mol. Struct. Res. 1 (1995) 1; http://www.cs.biu.ac.il:8080/∼hagit/papers/chemistry3.ps.Z.
[22] H. Zabrodsky, S. Peleg and D. Avnir, J. Am. Chem. Soc. 114 (1992) 7843.
[23] H. Zabrodsky, S. Peleg and D. Avnir, J. Am. Chem. Soc. 115 (1993) 8278–8289.